Short Communication

Imaging morphological details and pathological differences of red blood cells using tapping-mode AFM

A.S.M. Kamruzzahan[1], Ferry Kienberger[1], Cordula M. Stroh[1], Jörg Berg[2], Ralf Huss[3], Andreas Ebner[1], Rong Zhu[1], Christian Rankl[1], Hermann J. Gruber[1] and Peter Hinterdorfer[1,*]

[1] Institute of Biophysics, University of Linz, Altenbergerstr. 69, A-4040 Linz, Austria

[2] Institute for Medical Diagnostics and Immunologie, General Hospital of Linz, Krankenhaus Strasse 9, A-4020 Linz, Austria

[3] Institute of Pathology, University of Munich, Thalkirchner Str. 36, D-80337 Munich, Germany

*Corresponding author
 e-mail: peter.hinterdorfer@jku.at

Abstract

The surface topography of red blood cells (RBCs) was investigated under near-physiological conditions using atomic force microscopy (AFM). An immobilization protocol was established where RBCs are coupled via molecular bonds of the membrane glycoproteins to wheat germ agglutinin (WGA), which is covalently and flexibly tethered to the support. This results in a tight but non-invasive attachment of the cells. Using tapping-mode AFM, which is known as gentle imaging mode and therefore most appropriate for soft biological samples like erythrocytes, it was possible to resolve membrane skeleton structures without major distortions or deformations of the cell surface. Significant differences in the morphology of RBCs from healthy humans and patients with systemic lupus erythematosus (SLE) were observed on topographical images. The surface of RBCs from SLE patients showed characteristic circular-shaped holes with approx. 200 nm in diameter under physiological conditions, a possible morphological correlate to previously published changes in the SLE erythrocyte membrane.

Keywords: AFM; erythrocytes; imaging; molecular recognition; red blood cells; SLE.

AFM has been widely applied for imaging biological samples under physiological conditions (for a review see Hoerber and Miles, 2003). It has been shown that AFM yields high-resolution topography images of protein molecules, nucleic acids and biomembranes in their native, aqueous environment (e.g. reviewed by Engel and Mueller, 2000). However, there are several difficulties and limitations in studying soft cells which obscure high lateral resolution of cell-surface structure details, i.e. mainly tip-induced deformation of the soft cell surface and lateral displacement of the overall cell (Dufrene, 2001; Radmacher, 2002; Dvorak, 2003). In order to reduce the overall displacement during imaging, immobilization procedures for tight and non-invasive anchoring of cells to substrates have been developed (Schilcher et al., 1997). In addition, dynamic force microscopy (DFM) methods like tapping-mode (Putman et al., 1994) and MACmode AFM (Han et al., 1996) have greatly reduced the problem of lateral forces responsible for tip-induced deformation of soft biological samples (Kienberger et al., 2003).

DFM uses the dynamic properties of a Hookian spring to oscillate the cantilever at defined preset frequency and amplitude. In contrast to contact-mode AFM, where the tip mechanically contacts the sample permanently while it scans over the surface (Mueller et al., 1995), in DFM the cantilever touches the sample only at the end of its downward movement. Thus, the advantage of DFM is that lateral friction forces during imaging are significantly reduced, thereby minimizing sample damage by the scanning cantilever (Kienberger et al., 2004). Imaging of biological specimens has therefore significantly benefited from the development of DFM, since soft samples are less deformed and specimens weakly adhered to surfaces are not so easily displaced by the scanning cantilever (Kienberger et al., 2003).

For anchoring living cells to the substrate, flexible linkers are appropriate tools to achieve immobilization of cells by avoiding direct physical contact to the probe surface (Schilcher et al., 1997). The cells are thus anchored at a small distance from the surface, which may allow for unaffected cell physiology. Major tasks for the development of such binding protocols are the realization of defined and suitable coupling chemistry and the adjustment of the surface density of the linkers. Different strategies have been used so far for the specific and site-directed binding of biomolecules to surfaces (Wang et al., 2002; Hinterdorfer, 2002; Klein et al., 2003). Here we report on the attachment of red blood cells (RBCs) to mica surfaces for atomic force microscopy studies. Using tight and non-invasive immobilization of RBCs to mica surfaces via flexible linkers, fine structural details on the cell surfaces were resolved and major differences in the cell morphology of RBCs extracted from healthy volunteers and patients with systemic lupus erythematosus (SLE) were obtained in tapping-mode AFM topography images. Circular-shaped holes with diameters of ca. 200 nm were observed in the cell surface of RBCs derived from patients with SLE.

As the first step in anchoring RBCs to mica, the surfaces were amine-terminated by esterification of the sila-
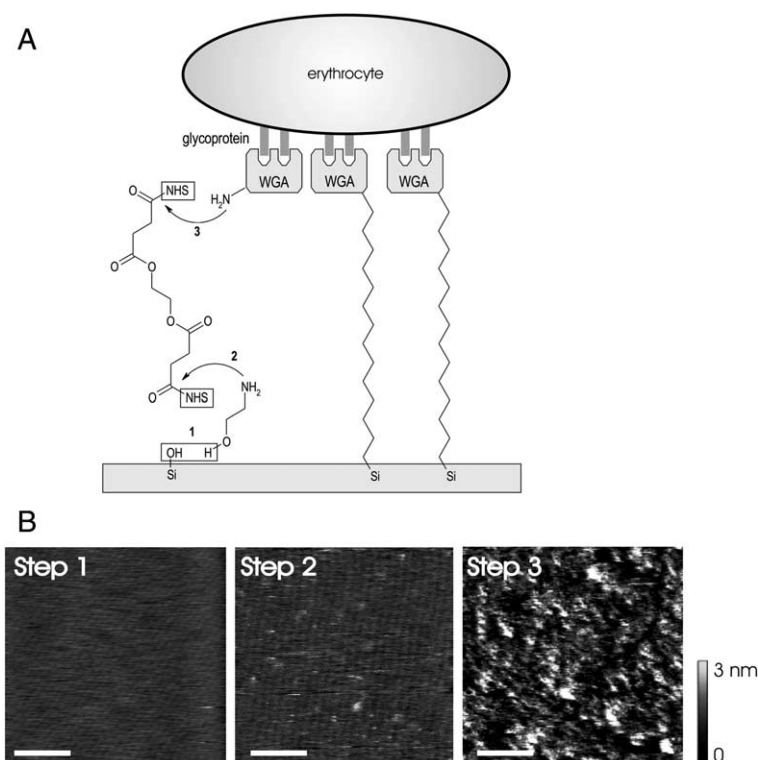
Figure 1 Surface chemistry.
(A) Scheme of erythrocyte immobilization via surface-bound lectin. Freshly cleaved mica sheets (10×10 mm) were incubated overnight in a solution of 6.6 g ethanolamine in 12 ml dimethylsulfoxide (DMSO) at 90°C in the presence of molecular sieve beads (0.3 nm; for details see Riener et al., 2003). After rinsing with DMSO and ethanol, the mica sheets were dried in a nitrogen stream (step 1). Amino-modified mica sheets were then immersed for 1 hour in a chloroform solution containing 1 mg/ml ethyleneglycol-bis(succinimidyl-succinate) (EGS, from Sigma, Vienna, Austria) and 0.5% (v/v) triethylamine, subsequently washed in chloroform, and dried in a nitrogen flow (step 2). In order to couple wheat-germ agglutinin (WGA) to the surface, 0.5 mg/ml WGA in phosphate-buffered saline (PBS; 150 mM NaCl, 5 mM NaH$_2$PO$_4$, pH 7.5) were placed on the mica sheets for 2 hours and finally washed with the same buffer (step 3). (B) Characterization of the modification steps using AFM. The surface topography after each step (cf. panel A) was obtained using dynamic force microscopy. In DFM the cantilever oscillation is maintained at constant amplitudes as the tip scans the sample surface. The reduction in oscillation amplitude is used as the feedback-control signal to measure the surface topography. All images shown in this study were taken with the dynamic force microscopy mode using a commercial fluid cell. Silicon nitride cantilevers (Veeco, Santa Barbara, USA) with nominal spring constants of 0.01 N/m were taken for imaging at 30 kHz oscillation frequency and 15 nm oscillation amplitude. The feedback loop was driven at 30% amplitude reduction. Images were acquired at scan rates of 2 lines/s with 256 pixel points per line. The total recording time per image was 2 min. Left panel: topographical image of the mica surface after esterification with ethanolamine (step 1). A flat surface with a roughness of ca. 0.4 nm is obtained. The scan size was 1×1 µm (scale bar: 250 nm). The height scale range is from 0 to 3 nm (see height bar). Middle panel: surface topography after reaction with the bifunctional crosslinker (step 2). The same scan size and height scale as before was used. Right panel: surface topography after covalent attachment of wheat-germ agglutinin (WGA). Several individual WGA molecules can be observed with about 20 nm in diameter and ca. 2 nm in height. Same scan size and height scale as before.

nol groups with ethanolamine (Figure 1A). The density of reactive amino groups created on mica was roughly 1000 groups/µm², as determined using an enzyme-immuno assay (Hinterdorfer et al., 1998). The esterification process results in flat surfaces with a roughness of approx. 0.4 nm (Figure 1B, step 1). The amines on the mica surface were allowed to react with a bifunctional crosslinker that contains two amino-reactive termini (NHS ester function). A high concentration of bis-NHS was used to avoid loop formation on the surface. In addition, for a fast reaction of NHS to amines and for preventing hydrolysis of the NHS residues, dry solvent and tertiary amine base conditions were applied (chloroform with triethylamine). According to the low molecular mass of the bifunctional crosslinker used, topographical images revealed that the surfaces remained smooth (Figure 1B, step 2).

The NHS-terminated surfaces prepared in this way were then used to covalently attach wheat-germ agglu-

tinin (WGA) molecules by formation of an amide bond between the NHS ester on the surface and a lysine group of WGA. The distribution of WGA proteins was fairly homogenous over the whole mica surface (Figure 1B, step 3). A high coverage was obtained and single WGA molecules were discernable with 20 nm in diameter and 2 nm in height; the overall surface roughness was increased thereby to ca. 2 nm (Figure 1B; identical height-scale for all three images). WGA is a plant lectin that was found to bind carbohydrate moieties of the glycocalix from red blood cells (Salzer et al., 2002). Thus, WGA covalently bound to mica was subsequently used as a functional matrix to specifically attach red blood cells via the carbohydrate moieties on their membrane surfaces. RBCs isolated from human donors were attached to the mica-bound WGA-matrix and fixed with glutaraldehyde.

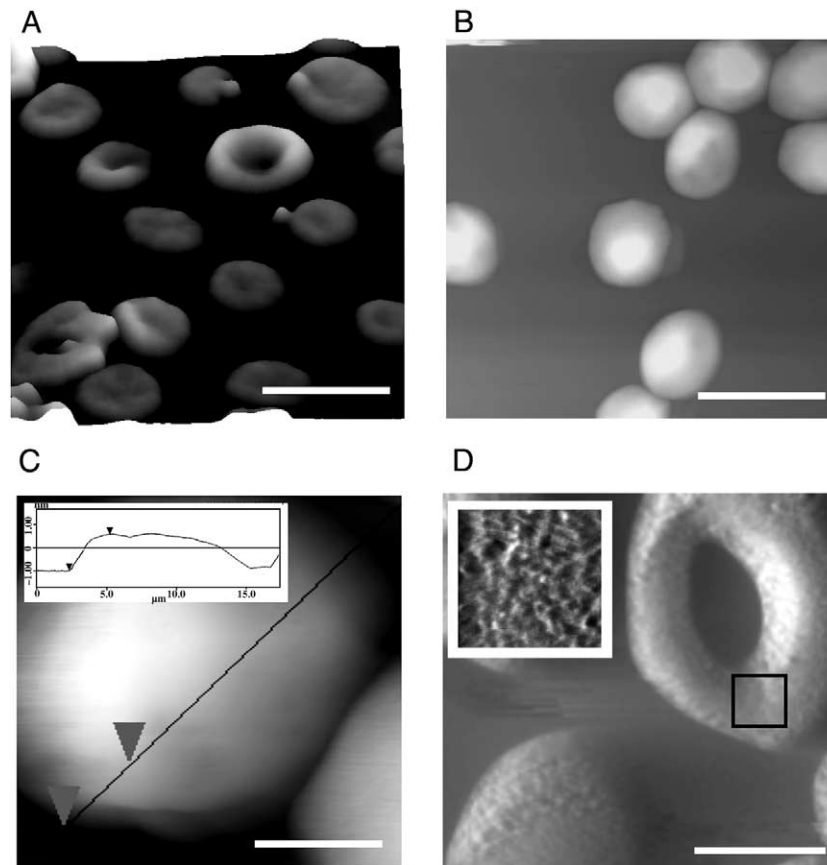The immobilized RBCs were imaged with tapping-mode AFM in buffer solutions. Using a soft (i.e. small

Figure 2   AFM images of RBCs from healthy humans specifically bound to a WGA matrix on mica.
Human red blood cells (RBCs) from healthy volunteers (Figure 2) or patients with systemic lupus erythematodes (Figure 3), respectively, were freshly prepared from EDTA-blood by 1:2 dilution in PBS followed by discontinuous density gradient centrifugation on Lymphoprep™ at 800 g for 30 min (Boyum, 1968). Subsequently, the supernatant including the density gradient was completely removed. The upper 1/3 of the red cell pellet (containing granulocytes) was also removed without disturbing the lower pellet. RBCs were washed once in PBS, resuspended in PBS, and celularity of the preparation was analyzed on an automated hematology analyzer (Sysmex SF 3000, Hamburg, Germany). RBC preparations contained always less than 0.5‰ white blood cells. For the binding of RBCs to the WGA-modified surface, RBCs were diluted 1:60 using PBS and adsorbed for 20 min on the mica sheets, followed by washing with PBS and fixation of immobilized RBCs with 1% glutaraldehyde for 1 min. After removal of the fixation agent by washing with the same buffer, AFM images (acoustic excitation with a multimode Nanoscope IIIa, Veeco) were acquired in a fluid cell at room temperature. (A) Topographical image showing that many immobilized cells are in a biconcave-shaped form. Scan area was 30×30 μm (scale bar: 10 μm). The height scale range is from 0 to 3 μm. (B) Topographical image of RBCs from a different healthy human exhibiting mostly globular-shaped cells. Scan size was 50×50 μm (scale bar: 15 μm). The height scale range is from 0 to 3 μm. (C) A single globular-shaped cell with a diameter of approx. 11 μm and a height of ca. 2 μm is shown. The scan size was 10×10 μm (scale bar: 4 μm). The height scale range is from 0 to 2 μm. The inset shows the cross-section profile along the solid line. (D) Smaller scan size image of a biconcave-shaped RBC showing a textured cell surface. The scan area was 10×10 μm (scale bar: 3 μm). The z-range is from 0 to 1 μm. The black square indicates the region for subsequent imaging. Inset: polygonal surface structures with heights of ca. 20 nm can be discerned on the cell surface at lower scan sizes (scan size was 2×2 μm; the z-range is from 0 to 50 nm).

spring constant) cantilever, the oscillation amplitude and the amplitude reduction during imaging were minimized to reduce the indentation force of the scanning tip (Kienberger et al., 2003). A careful adjustment of the imaging parameters during scanning is known to be essential for the successful imaging of thick and soft materials like whole cells (Vie et al., 2000).

Topographical images of RBCs from healthy humans are shown in Figure 2. The large-scale overview displays most of the erythrocytes in the expected biconcave-shaped form with dimensions of ca. 2 μm in height and 6–9 μm in diameter (Figure 2A). Since the cells remained stably bound during successive images, the immobilization of each single erythrocyte occurred probably via many WGA/carbohydrate bonds, due to the high surface density of both the WGA molecules at the surface and the sugars on the cell membrane. Erythrocytes appeared not only in biconcave form, but also in a spherical-shaped form with slightly larger dimensions (Figure 2B); the cross-section profile of a spherical-shaped cell shows a diameter of approx. 11 μm (Figure 2C). Several mechanisms were suggested leading to the swollen appearance of the RBCs (Girasole et al., 2001). Most likely, the cytoskeleton, i.e. the underlying protein structure in the cytoplasm of the cell, is weakened and hence the normal biconcave nature of the cell is changed to the thermodynamically more favorable spherical forms of this type of morphology (Nowakowski et al., 2001). In order to demonstrate that the spherical form of the RBCs does not arise from the fixation process, living cells were immobilized in the same way and imaged without glutaraldehyde treatment (data not shown). Indeed, a similar
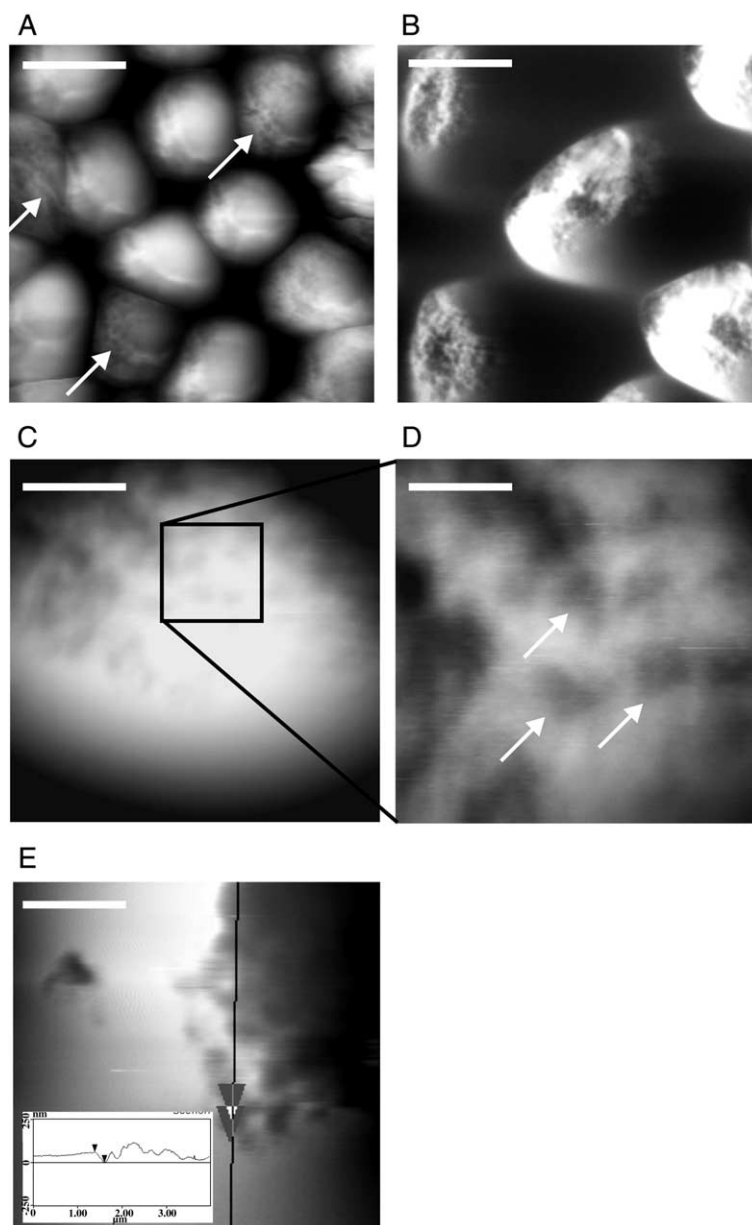
Figure 3 AFM images of RBCs derived from patients with systemic lupus erythematosus (SLE).
(A) Large-scale overview of RBCs showing various corrugations and holes. Arrows indicate cells where holes are discernable. The scan area was 30×30 μm (scale bar: 10 μm). The height scale range is from 0 to 2.5 μm. (B) Topographical image of RBCs exhibiting major morphological deformations like crater-like structures with depths of approx. 1 μm and granularly arranged holes. The scan size was 20×20 μm (scale bar: 7 μm). The height scale range is from 0 to 3 μm. (C) A single RBC with various corrugations and holes. Scan size was 4×4 μm (scale bar: 1 μm). The height scale range is from 0 to 500 nm. (D) Smaller scan area image with a dense arrangement of holes (marked with arrows). The scan size was 2×2 μm (scale bar: 700 μm). The height scale range is from 0 to 100 nm. (E) The cross-section profile (inset) along the solid line shows the dimensions of holes, i.e. diameters of about 200 nm and depths of ca. 80 nm. The scan area was 4×4 μm (scale bar: 1 μm). The height scale range is from 0 to 500 nm.

globular appearance of erythrocytes was observed, indicating that the fixation process did not significantly alter the morphology of RBCs (Swihart et al., 2001; Touhami et al., 2002). In higher magnification images, fine substructural details of the cell surface were revealed (Figure 2D). The small scan area image of the cell surface showed approx. 200 nm sized patterns with heights of ca. 20 nm (Figure 2D, inset); these structures most likely reflect features from the underlying cytoskeleton of the cell (Nowakowski et al., 2001). The features identified here compare nicely to the known cytoskeleton network of spectrin molecules (Takeuchi et al., 1998).

Topographical images of red blood cells extracted from patients with systemic lupus erythematosus (SLE) are shown in Figure 3. SLE is an autoimmune disease characterized by anti-DNA autoantibodies and circulating immune complexes (Lorenz et al., 2001). Chromosomal DNA and other nucleic acids involved in SLE are usually cleared from blood circulation by binding to a yet unidentified receptor-like protein on the surface membrane of erythrocytes. RBCs derived from SLE patients show an overall reduced binding capability and pre-saturated binding kinetics of DNA to the cell surface (Huss et al., 2000). Autoantibodies and DNA bound to the surface of

erythrocytes lead to the activation of the macrophage system, and macrophage-mediated erythro-phagocytosis has been observed (Brentjens et al., 1975; Weidner and Lorentz, 1986; Huss et al., 2000).

One aim of this study was to investigate possible morphological differences of erythrocytes from healthy and SLE-affected individuals using AFM. Indeed, topographical images of RBCs derived from humans with SLE, generated using the same immobilization procedure as before, show various differences in cell morphology (Figure 3). On a large-scale overview several erythrocytes with various corrugations (Figure 3A, arrows) and crater-like deformations affecting the cell appearance to a large extent are observed (Figure 3B). Reducing the image area revealed a more detailed view of the pathological surface structures. In Figure 3C, several holes and corrugations were observed. A fairly dense arrangement of circular-shaped hole scan be seen in Figure 3D (marked with arrows). According to the cross-section profile along a corrugated RBC (Figure 3E), the holes have diameters of approx. 200 nm.

The features observed in the topography of RBC derived from patients with SLE may give additional insights into the development of the disease. The holes and corrugations observed might be responsible for the reduced binding capability and pre-saturated binding kinetics of DNA to the cell surface, as observed by Huss et al. employing macroscopic binding assays of RBCs derived from SLE patients (Huss et al., 2000). In addition, similar pathological changes on macroscopic cell tissues from humans with SLE were found using immuno-fluorescence studies (Brentjens et al., 1975), which might be associated with already described functional deficiencies of red blood cells in SLE (Cohen et al., 1999; Richaud-Patin et al., 2003).

In conclusion, the methodology of immobilization described here results in a stable and non-destructive anchoring of red blood cells to a WGA matrix. Since almost every cell contains extracellular carbohydrate moieties, the immobilization protocol may serve as a general strategy to immobilize various cell types for AFM experiments. RBCs were imaged by dynamic force microscopy at low forces under near-physiological conditions, revealing sub-structural details of the cell membrane. On RBCs derived from patients with SLE, various morphological features like tubular holes and crater-like deformations were observed.

Acknowledgments

References

Boyum, A. (1968). Separation of leucocytes from blood and bone marrow. Scand. J. Clin. Lab. Invest. (Suppl.) *97*, 9–29.

Brentjens, J.R., Sepulveda, M., Baliah, T., Bentzel, C., Erlanger, B.F., Elwood, C., Montes, M., Hsu, K.C., and Andres, G.A. (1975). Interstitial immune complex nephritis in patients with systemic lupus erythematosus. Kidney Int. *7*, 342–350.

Cohen, J.H., Atkinson, J.P., Klickstein, L.B., Oudin, S., Subramanian, V.B. and Moulds, J.M. (1999). The C3b/C4b receptor (CR1, CD35) on erythrocytes: methods for study of the polymorphisms. Mol. Immunol. *36*, 819–825.

Dufrene, Y.F. (2001). Application of atomic force microscopy to microbial surfaces: from reconstituted cell surface layers to living cells. Micron *32*, 153–165.

Dvorak, J.A. (2003). The application of atomic force microscopy to the study of living vertebrate cells in culture. Methods *29*, 86–96.

Engel, A., and Muller, D.J. (2000). Observing single biomolecules at work with the atomic force microscope. Nat. Struct. Biol. *7*, 715–718.

Girasole, M., Cricenti, A., Generosi, R., Congiu-Castellano, A., Boumis, G., and Amiconi, G. (2001). Artificially induced unusual shape of erythrocytes: an atomic force microscopy study. J. Microsc. *204*, 46–52.

Han, W., Lindsay, S.M., and Jing, T. (1996). A magnetically driven oscillating probe microscope for operation in liquid. Appl. Phys. Lett. *69*, 1–3.

Hinterdorfer, P. (2002). Molecular recognition studies using the atomic force microscope. Methods Cell Biol. *68*, 115–139.

Hinterdorfer, P., Schilcher, K., Baumgartner, W., Gruber, H.J., and Schindler, H. (1998). A mechanistic study of the dissociation of individual antibody-antigen pairs by atomic force microscopy. Nanobiology *4*, 177–188.

Horber, J.K., and Miles, M.J. (2003). Scanning probe evolution in biology. Science *302*, 1002–1005.

Huss, R., Haas, C., Herrmann, M., Kalden, J.R., and Loehrs, U. (2000). Impairment of genomic DNA binding to a putative dysfunctional receptor on erythrocytes independent of complement and antibodies in systemic lupus erythematosus. Virchow's Arch. *437*, 380–387.

Kienberger, F., Stroh, C., Kada, G., Moser, R., Baumgartner, W., Pastushenko, V., Rankl, C., Schmidt, U., Muller, H., Orlova, E. et al. (2003). Dynamic force microscopy imaging of native membranes. Ultramicroscopy *97*, 229–237.

Kienberger, F., Zhu, R., Moser, R., Rankl, C., Blaas, D., and Hinterdorfer, P. (2004). Dynamic force microscopy for imaging of viruses under physiological conditions. Biol. Proced. Online *6*, 120–128.

Klein, D.C., Stroh, C.M., Jensenius, H., van Es, M., Kamruzzahan, A.S., Stamouli, A., Gruber, H.J., Oosterkamp, T.H., and Hinterdorfer, P. (2003). Covalent immobilization of single proteins on mica for molecular recognition force microscopy. ChemPhysChem *4*, 1367–1371.

Lantz, M., Liu, Y.Z., Cui, X.D., Tokumoto, H., and Lindsay, S.M. (1999). Dynamic force microscopy in fluids. Interface Anal. *27*, 354–360.

Lorenz, H.M., Herrmann, M. and Kalden, J.R. (2001). The pathogenesis of autoimmune diseases. Scand. J. Clin. Lab. Invest. (Suppl.) *235*, 16–26.

Muller, D.J., Schabert, F.A., Buldt, G., and Engel, A. (1995). Imaging purple membranes in aqueous solutions at sub-nanometer resolution by atomic force microscopy. Biophys. J. *68*, 1681–1686.

Nowakowski, R., Luckham, P., and Winlove, P. (2001). Imaging erythrocytes under physiological conditions by atomic force microscopy. Biochim. Biophys. Acta *1514*, 170–176.

Putman, C.A.J., Vanderwerf, K.O., de Grooth, B.G., Vanhulst, N.F., and Greve, J. (1994). Tapping mode atomic force microscopy in liquid. Appl. Phys. Lett. *64*, 2454–2456.

Radmacher, M. (2002). Measuring the elastic properties of living cells by the atomic force microscope. Methods Cell Biol. *68*, 67–90.

Richaud-Patin, Y., Perez-Romano, B., Carillo-Maravilla, E., Rodriguez, P., Simon, A.J., Cabiedes, J., Jakez-Ocampo, J., Llorente, L. and Ruiz-Arguelles, M. (2003). Deficiency of red cell bound CD55 and CD59 in patients with systemic lupus erythematosus. Immunol. Lett. 88, 95–99.

Salzer, U., Hinterdorfer, P., Hunger, U., Borken, C., and Prohaska, R. (2002). Ca^{2+}-dependent vesicle release from erythrocytes involves stomatin-specific lipid rafts, synexin (annexin VII), and sorcin. Blood *99*, 2569–2577.

Schilcher, K., Hinterdorfer, P., Gruber, H. J., and Schindler, H. (1997). A non-invasive method for the tight anchoring of cells for scanning probe microscopy. Cell Biol. Int. *21*, 769–778.

Swihart, A.H., Mikrut, J.M., Ketterson, J.B., and Macdonald, R.C. (2001). Atomic force microscopy of the erythrocyte membrane skeleton. J. Microsc. *204*, 212–225.

Takeuchi, M., Miyamoto, H., Sako, Y., Komizu, H., and Kusumi, A. (1998). Structure of the erythrocyte membrane skeleton as observed by atomic force microscopy. Biophys. J. *74*, 2171–2183.

Touhami, A., Othmane, A., Ouerghi, O., Ben Ouada, H., Fretigny, C., and Jaffrezic-Renault, N. (2002). Red blood cells imaging and antigen-antibody interaction measurement. Biomol. Eng. *19*, 189–193.

Vie, V., Giocondi, M.C., Lesniewska, E., Finot, E., Goudonnet, J.P., and Le Grimellec, C. (2000). Tapping-mode atomic force microscopy on intact cells: optimal adjustment of tapping conditions by using the deflection signal. Ultramicroscopy *82*, 279–288.

Wang, H., Bash, R., Yodh, J.G., Hager, G.L., Lohr, D., and Lindsay, S.M. (2002). Glutaraldehyde modified mica: a new surface for atomic force microscopy of chromatin. Biophys. J. *83*, 3619–3625.

Weidner, N., and Lorentz, W. B. (1986). Scanning electron microscopy of the acellular glomerular and tubular basement membrane in lupus nephritis. Am. J. Clin. Pathol. *85*, 135–145.